Biosensors and Bioelectronics 179 (2021) 113053

Contents lists available at ScienceDirect

Biosensors and Bioelectronics

journal homepage: http://www.elsevier.com/locate/bios

Binary mixture quantification using cell-based odor biosensor system with active sensing

Yuji Sukekawa [a,1], Hidefumi Mitsuno [b], Ryohei Kanzaki [b], Takamichi Nakamoto [a,*]

[a] Laboratory for Future Interdisciplinary Research of Science and Technology (FIRST), Institute of Innovative Research (IIR), Tokyo Institute of Technology, 4259 Nagatsuta-cho, Midori, Yokohama, Kanagawa, 226-8503, Japan
[b] Research Center for Advanced Science and Technology (RCAST), The University of Tokyo, 4-6-1 Komaba, Meguro, Tokyo, 153-8904, Japan

ARTICLE INFO

Keywords:
Odor biosensor
Cell-based sensor
Image processing
Active sensing
Quantification

ABSTRACT

Organisms perceive odorants in the environment through the use of a large number of olfactory receptors. Various odor biosensors have been researched and developed in order to mimic this olfactory mechanism. This study examines the quantification of odorant concentrations through the use of a sensor array comprised of several types of cell-based odor sensors expressing insect olfactory receptors with nonlinear characteristics. The sensor system utilized an active sensing method in order to compare the responses of a target odorant and a prepared odorant in determining the relative concentration of the target odorant. By combining an active sensing method with a real-time reference method in which the target odorant was measured every time the prepared odorant was measured, the relative concentrations were successfully determined even when the response fluctuation was large or odorant sensor cell responses varied as measurement time increased. For proof of concept purposes, the study primarily focused on quantifying odorant concentrations composed of one or two odorant components. It was confirmed that an algorithm to find the optimal relative odorant concentration among a limited number of odorant concentrations is achievable. Though this study is still in the initial stage of the developing odor sensors and has many challenges, it can provide insight into paving the way towards a new type of odor biosensor with active sensing.

1. Introduction

While odors are invisible, they are used in a variety of diverse situations to provide different kinds of information. For example, animals use olfaction in order to make decisions about food freshness and deterioration, and there is evidence that body odor may reflect one's health condition (Olsson et al., 2014). Furthermore, smell is evocative; you may have felt pleasure after sniffing a nostalgic smell that you wanted to keep forever. There has been substantial research on developing methods for artificial olfaction. This has the potential for improvements in many applications including food and flavor manufacturing, explosive detection, and simple disease diagnosis. Also, the development of odor recording devices, akin to cameras and microphones that record sight and audio, serves as an interesting prospect in the field of artificial olfaction.

However, challenges persist with developing robots or machines that can achieve olfaction. Research regarding electronic noses have been carried out for several decades. An electronic nose traditionally refers to a sensor array composed of multiple sensor elements in which the sensor array response is used in pattern recognition to classify odorants (Gutierrez-Osuna, 2002; Hsieh and Yao, 2018; Marco and Gutierrez-Galvez, 2012). Based on the idea that animals have multiple types of olfactory receptors to recognize odors, this type of method attempts to mimic actual animal olfaction systems. However, traditional electronic noses rely on artificial sensor materials such as metal oxide and conducting polymer that are intrinsically different from biological elements such as olfactory receptors. Therefore, an odor biosensor that uses actual animal olfactory receptors becomes a possible solution in developing artificial noses.

Currently, research regarding odor biosensors that use biomaterials such as olfactory receptor neurons and receptor proteins is rapidly progressing. These sensors are sometimes called bioelectronic noses,

* Corresponding author.
E-mail addresses: sukekawa@brain.imi.i.u-tokyo.ac.jp (Y. Sukekawa), mitsuno@brain.imi.i.u-tokyo.ac.jp (H. Mitsuno), kanzaki@rcast.u-tokyo.ac.jp (R. Kanzaki), nakamoto.t.ab@m.titech.ac.jp (T. Nakamoto).
[1] Current address: Research Center for Advanced Science and Technology (RCAST), The University of Tokyo, 4-6-1 Komaba, Meguro, Tokyo 153–8904, Japan.

https://doi.org/10.1016/j.bios.2021.113053
Received 31 August 2020; Received in revised form 17 January 2021; Accepted 27 January 2021
Available online 31 January 2021

which use several transducers such as quartz crystal microbalances (Ko and Park, 2005; Sung et al., 2006), surface acoustic wave devices (Olsson et al., 2015; Wu et al., 2011), and field effect transistors (Murugathas et al., 2019; Son et al., 2017), or utilize analytical methods such as light addressable potentiometric sensors (Liu et al., 2010), electrochemical impedance spectroscopy (Khadka et al., 2019), and fluorescent imaging (Figueroa et al., 2010; Lee et al., 2015). Advantages of these sensors are mainly sensitivity and selectivity, owing to the specificity of biological materials. In other words, by using olfactory materials, the odor biosensors make it possible to detect what the traditional electronic noses are not able to do.

While these odor biosensors are suitable for detection of specific odorants with high sensitivity and selectivity, they are limited in the number of olfactory receptors and odors that they can detect. However, odorants in the world are normally a mixture of chemical components in which the composition of some odorants remain unknown. When designing odor biosensors, it is essential to develop a sensor array with multiple olfactory receptors that can measure arbitrary odorants in order to reflect the real-world situation.

Previous research relating to the measurement of odorants in the natural environment include odorant mixture quantification. Conventional mixture quantification is based on linear methods such as multiple linear regression and partial least squares regression (Carey et al., 1987; Vergara et al., 2007) and non-linear methods using artificial neural networks such as multi-layer perceptron (Sundgren et al., 1991; Wang et al., 1995). The sensing elements in these conventional studies are artificial sensors including metal-oxide gas sensors and quartz resonator sensors. Comparing to linear methods, non-linear methods generally have a relatively high accuracy for mixture quantification as artificial gas sensors have non-linear characteristics. However, non-linear methods require more data points to build the quantification model and are not robust against temporal property change such as sensor drift and aging.

Furthermore, odor recorders have also been used for odorant measurement (Nakamoto, 2016). Odor recorders measure odorants by using sensor arrays comprised of artificial sensors and quantify the composition of odorants in order to reproduce odorants. Yamanaka et al. (2003) is known for one such odor recorder in which we utilized an active sensing method for quantification. Active sensing is one measurement technique that can extend the capability of measurable range by dynamically controlling the system itself. When quantifying odorant concentrations, it is difficult to measure the unknown odorant concentration as an absolute value. To combat this, the system using active sensing simplifies the quantification as a relative comparison between odorant responses to a known and an unknown odorant concentration in which the measurable range is extended. Active sensing allows the influence of sensor fluctuation to be reduced and removes the need for a calibration process. Furthermore, the collinearity problem is described as multicollinearity between sensor array responses in which the robustness of the regression result against data fluctuation deteriorates. In our previous study (Yamanaka et al., 2003), quartz resonator sensors were used and the collinearity problem limited the capability for quantification.

A cell-based odor biosensor that utilized a fluorescent image as a sensor array was previously developed in order to classify odorants (Sukekawa et al., 2019). This study continued the development of our cell-based odor biosensor in which mixture quantification was carried out, extending previous research on mixture quantification of odor recorders. Odor biosensors are promising due to high selectivity and sensitivity and can avoid the problem of collinearity. Utilizing odorant biosensor for odorant quantification is a novel method.

However, additive property is not valid, and its behavior is nonlinear in odor biosensors. Moreover, sensor response fluctuates more than artificial sensors. Therefore, it is difficult to create a model that can quantify mixtures. In order to avoid this problem, an active sensing method was proposed in this study to quantify mixture's composition using an odor biosensor. As measurement is relative, a model building procedure was not required. Furthermore, a real-time reference method (Yamanaka and Nakamoto, 2003) was used in active sensing to reduce the influence of sensor response fluctuation. This is the first report of mixture quantification using an odor biosensor with active sensing in which a binary mixture was successfully quantified. This proposed biosensor system can be used in the quantification of mixtures with a larger number of components or real sample analysis in the future. A summary table comparing previous works to this study is provided in Table S1 (Supplementary data).

2. Material and methods

2.1. Sensor cells, odorants, and a sensor array

In this study, odorant sensor cells (Mitsuno et al., 2015; Termtanasombat et al., 2016) comprised of insect Sf21 cells expressing insect olfactory receptors, olfactory receptor co-receptors (Orco), and calcium indicator fluorescent proteins (GCaMP6s) were used as odor biosensor elements. For a brief explanation, the odorant sensor cells were established by transfecting two expression vectors; pIB/V5-His vector (Invitrogen™) containing olfactory receptor gene and *Orco* gene and pIZ/V5-His vector (Invitrogen™) containing *GCaMP6s* gene (Chen et al., 2013). The cells were cultured in Grace's insect medium (Gibco™) with antibiotics (Blasticidin S and Zeocin) at 27 °C until use. The basic mechanism of an odorant sensor cell is described below. When the olfactory receptor binds to an odorant molecule, a cation channel composed of an olfactory receptor and a co-receptor opens and allows for calcium ion influx. As the odorant sensor cell includes fluorescent proteins, this allows for the change in calcium to be visualized through fluorescent imaging. The fluorescent image can then be considered as the sensor array output. Furthermore, the response characteristics of the odorant sensor cells depend on the olfactory receptors that are expressed in the cells. Therefore, multiple types of odorant sensor cells can be prepared easily. This study focused on two types of olfactory receptors, Or13a and Or56a which are derived from *Drosophila melanogaster*. The response characteristics of these receptors are reported (Galizia et al., 2010; Münch and Galizia, 2016; Stensmyr et al., 2012). Or13a is a broadly tuned receptor and strongly responds to 1-octen-3-ol. Or56a is narrowly tuned receptor and has a specific response to geosmin. Limit of detection has been reported in previous research (Mujiono et al., 2017). Sensor cells expressing Or13a and Or56a can detect 50 nM 1-octen-3-ol and 100 nM geosmin, respectively.

Based on the above, 1-octen-3-ol (O5284, Sigma-Aldrich) and geosmin (077–01911, Wako) were used as the odorant samples. For the preparation of the odorant sample solutions, odorants were first dissolved into dimethyl sulfoxide (DMSO; 043–07216, Wako) and diluted with modified Ringer's solution (140 mM NaCl, 5.6 mM KCl, 4.5 mM $CaCl_2$, 11.26 mM $MgCl_2$, 11.32 mM $MgSO_4$, 5 mM HEPES, and 9.4 mM D-glucose, pH 7.2). This resulted in a 100 μM (DMSO 0.1% v/v) 1-octen-3-ol solution and a 1 μM (DMSO 0.1% v/v) geosmin solution. In addition, an assay buffer solution consisting of modified Ringer's solution with 0.1% (v/v) DMSO was prepared.

The method used to construct a sensor array with the odorant sensor cells is the same as previously reported in (Sukekawa et al., 2019). In brief, multiple types of odorant sensor cells are mixed and put into a measurement chamber. Arrangement of these sensor cells are completely random. The fluorescent image contains response from each cell in which the image has a specific pattern corresponding to each odorant. The advantage of this sensor array is that the sensor array can be constructed with same sequence even if the number of olfactory receptor types are increased.

2.2. Measurement system

In order to measure the fluorescent image responses to odorants, an

odorant flow supply system that includes a handmade measurement chamber, and an optical measurement system were utilized. Fig. 1 shows the structure of the measurement chamber and odorant flow supply system. The measurement system was designed to enhance the robustness against the air bubbles encountered frequently in the previous system (Sukekawa et al., 2019). The measurement chamber was made of polydimethylsiloxane (PDMS; SILPOT 185, Dow Corning Toray). PDMS is a material usually used for microfluidic devices, though our measurement chamber does not have microfluidic channel. PDMS technique was adopted for rapid prototyping of the measurement chamber. The measurement chamber has a single 3 mm wide flow channel and two syringe pumps (Legato111, kdScientific) connected to the inlet and outlet of the flow channel via PTFE tubes.

In order to establish directional flow, an upstream pump infused the assay buffer and a downstream pump was used to withdraw the buffer. The flowrate was set to 100 μL/min. The rationale for the use of two syringe pumps was made on the fact that the flow channel requires a window portion to be exposed to the atmosphere in order to supply the odorant sample solution. To supply the odorant sample solution, a dispensing pump (LPDA2720125D, The Lee Company) first injects the sample solution into the micro dispensers (INKA2438510H, The Lee Company) installed above the channel window. When an electrical pulse is applied to a micro dispenser, the dispenser ejects droplets corresponding to the number of electrical pulses. In other words, the number of ejected droplets increases in proportion to the frequency of the driving signal. The droplets from the micro dispensers are then mixed with the assay buffer flow and finally reach the odorant sensor cells. Though there is some difficulty in deriving a precise final concentration as the droplets are not evenly mixed with assay buffer, an approximate concentration roughly corresponds to the volume of the supplied odorant solution. Therefore, it can be said that the concentration of odorant stimulus to the odorant sensor cells can be indirectly controlled by changing the driving frequency of the micro dispenser. In addition, multiple micro dispensers can be used to drop different odorant samples into the measurement chamber at the same time in order to measure responses as an odorant mixture. In this study, two sets of micro dispensers and dispensing pumps were used to match the two types of odorant samples.

Odorant sensor cells were injected into the channel of the measurement chamber by using a micro pipet and immobilized with physical adsorption to the bottom side of channel downstream to the window portion. An image sensor (OV7740, OmniVision) takes fluorescent images of sensor cells from bottom side of the chamber. The number of cells in the image region was approximately 200–300. When the number of cells is insufficient, the influence of response fluctuation among individual cells becomes large. On the other hand, when the number of cells is too much, only a part of cells can detect odorants, especially at low concentrations, and the response fluctuation of the sensor array also becomes large. For this reason, 200–400 cells was deemed to be an appropriate amount. An excitation light from a laser diode module (25 mW, 488 nm, NDS1306, Nichia) is applied to the sensor cells through optical modules. Though measurement using fluidic devices usually have problems related to air bubbles, our measurement chamber can suppress any air bubble interference as the air bubble is trapped to the window portion of the channel and cannot flow downstream.

2.3. Evaluation of sensor cell responses

As mentioned above, though the response of the sensor array with odorant sensor cells is a fluorescent image itself, it is necessary to

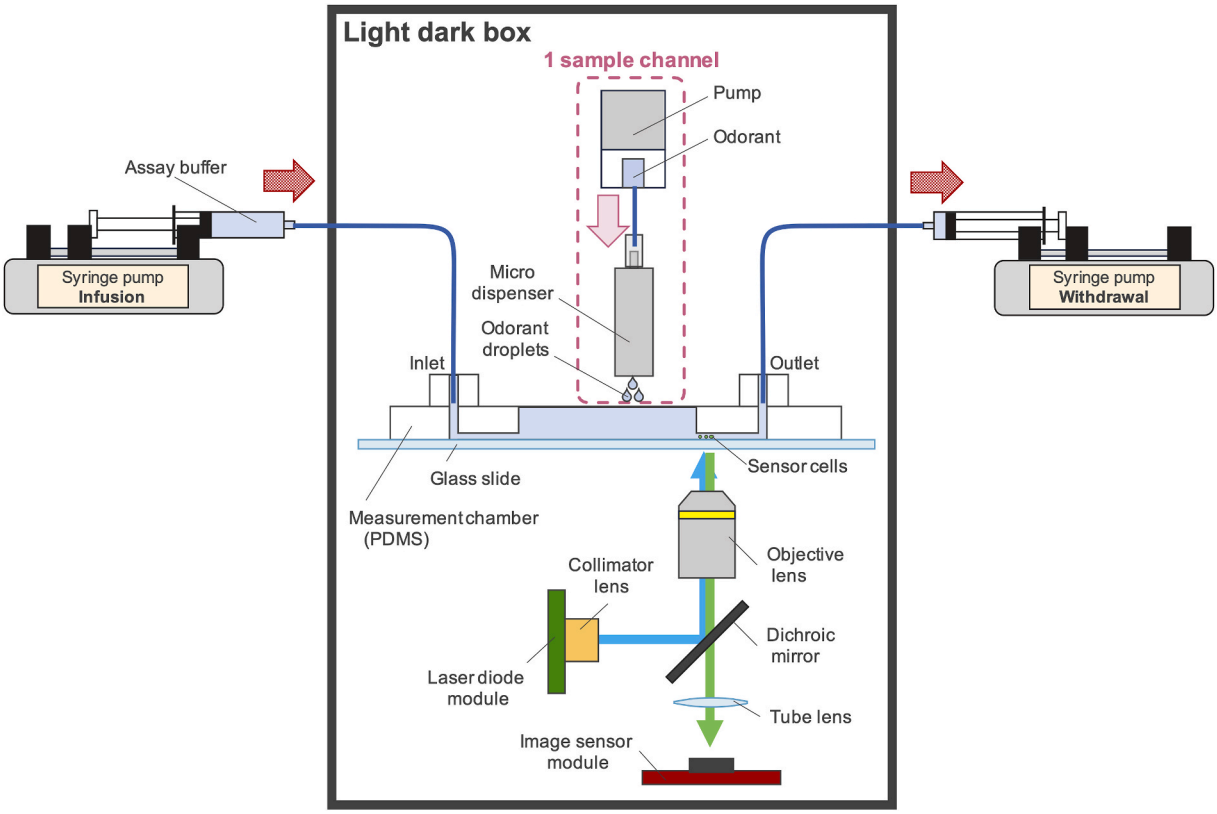

Fig. 1. Schematic view of the measurement chamber, the odorant sample supply system, and the optical measurement system. The odorant sensor cells were seeded into the measurement chamber made of PDMS. The cells were injected from the window portion of the measurement chamber by using a micro pipet and were dispersed to the bottom side of channel downstream to the window portion. The odorant stimulus was applied to the odorant sensor cells through first injecting the assay buffer solution using syringe pumps and dripping the odorant sample solution using micro dispensers. The responses of the sensor cells were taken as a fluorescent image by using an image sensor module.

convert to an appropriate format in order to compare the fluorescent images by odorant. Therefore, image processing to extract the temporal responses for each individual cell from the fluorescent image was carried out. This was previously reported in (Sukekawa et al., 2019). The image processing procedure is briefly described below. First, circle regions corresponding to the sensor cell areas are extracted from a fluorescent image by using circular Hough transform. Following this, the average pixel brightness value for each extracted cell area is calculated. The cell area extraction and the calculation of the average brightness are performed every sampling cycle after taking a fluorescent image. Furthermore, each sensor cell area is tracked by matching the cell area in the previous image to the area in the current image, so that the temporal responses for each sensor cell can be acquired. This resulted in approximately 200–400 temporal cell responses.

A sensor cell's response to odorants can be visualized when an odorant molecule binds to the olfactory receptor, giving off fluorescent intensity in a surge-like manner. Once the fluorescent intensity reaches peak point, it gradually goes back to the baseline. The change in the fluorescent intensity is the most important indicator representing odorant response. Thus, it is reasonable to evaluate the change in the response peak intensity relative to the response baseline as the sensor cell response. However, the peak responses of different olfactory receptors to different odorant stimuli (e.g. geosmin or 1-octen-3-ol) do not occur simultaneously. To mitigate this, relative fluorescent intensity change can be evaluated after a certain period of time following odorant stimulus application. This allows the change in intensity to be easily compared even if the types of odorant samples are different. Therefore, in this study, the relative change in fluorescent intensity for each sensor cell was evaluated at 60 s following odorant stimulus application and considered to be the sensor cell response regardless of the type of odorant sample used or its supply duration. The duration of 60 s was empirically selected, though it should be noted that the evaluation did not always match with the peak response. However, even if a sensor cell's 60 s response was not the peak response, this was not considered a problem as responses were compared using the same time evaluation criteria.

The image processing and evaluation of sensor cell responses should be performed in real time in which the quantification of odorant component concentration is described below. Therefore, a system that conducts real-time image processing was implemented into SoC FPGA chip including an ARM CPU core embedded in a PCB board (DE1-SoC, Terasic Inc.). The output from the image sensor in Fig. 1 was transferred to the ARM CPU and processed by a program running on the CPU, in which the response vector was output as the sensor response. The PCB board was able to control the odorant sample supply system as depicted in Fig. 1.

2.4. Active sensing and odorant quantification

In order to determine the concentration of an odorant using an odor

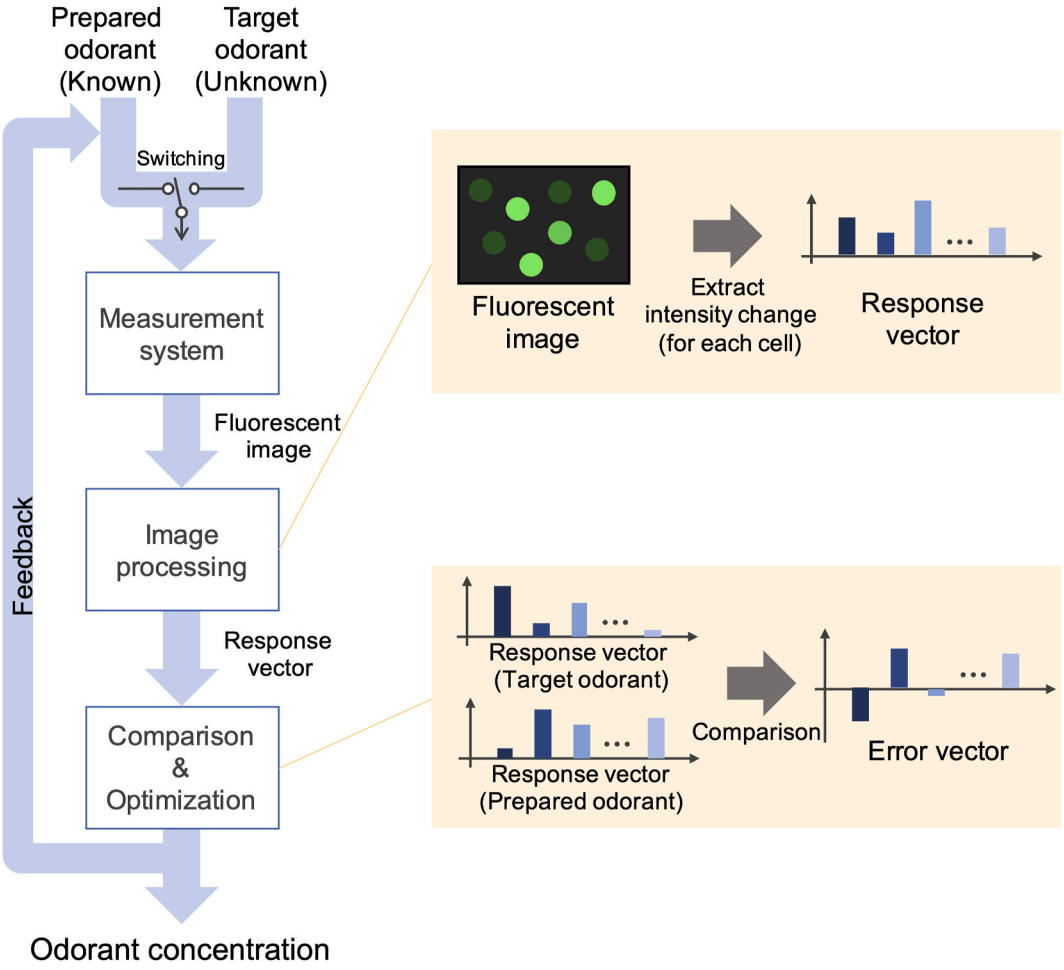

Fig. 2. Measurement principle and procedure for the quantification of odorant components concentration using active sensing. The fluorescent image acquired by the measurement system was processed to obtain the response vector as multi-dimensional temporal response. In addition, the response vector of the target odorant was evaluated and compared with that of the prepared odorant in which error information was fed back to the prepared odorant concentration for the next measurement. This procedure was repeated numerous times to bring the prepared odorant concentration closer to the target odorant concentration.

sensor, a calibration curve is usually obtained in which the unknown concentration is determined based on the response values of an odorant. However, odor sensors are often affected by changes in the measurement environment, leading to large fluctuations in sensor output data. In addition, it is often unfeasible to perform practical calibration of biosensors as output fluctuations of sensor elements are generally large.

Active sensing enhances the sensing capability by controlling the sensor system and dynamically changing the system to an appropriate state in relation to the measurement target. Odorant quantification is simplified into a relative comparison between odorant responses to a known and an unknown concentration. This allows the measurable range to be extended.

Fig. 2 depicts the flow of measurement for the quantification of the odorant concentrations. First, the system measures the response to an odorant of an unknown concentration (target odorant) and an odorant of known concentration (prepared odorant). Then, the obtained fluorescent images are processed in order to calculate the odorant response vectors. The system compares the odorant response vectors of the target odorant and the prepared odorant and feeds back the error information to modify the concentration of the next prepared odorants. By repeating this process several times, when the error is sufficiently small and the concentration between the prepared odorant and the target odorant can be considered equal from the view of the measurement system, the concentration of the target odorant can be determined. This approach is advantageous as in principle, it does not require calibration.

Odorant concentrations of the target odorant are unknown if odorant concentrations of the prepared odorants are unknown. However, it is still acceptable since our ultimate goal is to develop an odor recorder to replicate the odor regardless of odorant concentration information. Moreover, odorant quantification is available only when the prepared odorants contain the target odorants. On the other hand, if the prepared odorants do not contain the target odorants, the system attempts to make the prepared odorants similar to the target odorants. In other words, the system approximates the target odorants by using the prepared odorants. This operation then becomes odorant recording rather than odorant quantification in which the system is able to record even unknown odorants. Therefore, though we demonstrated odorant quantification in this study, the system is also able to record odors.

A previous study regarding odorant concentration quantification using active sensing has been conducted using a sensor array of quartz crystal microbalances (Yamanaka et al., 2003). This study succeeded in quantifying the concentrations of multiple odorant components. Furthermore, a method termed real-time reference method was reported in Yamanaka and Nakamoto (2003) in order to reduce the influence of environmental fluctuation during measurement. Though ideally the target odorant response should be measured only once, this method mitigates any fluctuation in the target odorant response by re-measuring the target odorant before every measurement of the prepared odorant.

2.5. Odorant quantification algorithms

This study focused on specifically measuring one or two components in an odorant to quantify the odorant concentrations. To account for the measurement resolution of the odor biosensor, the target odorant and the prepared odorant were limited to only a specific range of concentrations. In other words, as the odorant concentrations can be indirectly controlled by the micro dispenser's driving frequency, the concentrations of the target odorant and the prepared odorant were controlled based on selecting different driving frequencies. Depending on whether one or two odor components were quantified, different quantification algorithms were used.

In the case of a single component odorant concentration quantification, the micro dispenser driving frequency for the odorant supply were 0, 10, 30, 100, and 300 Hz, with one driving frequency being the concentration of the target odorant and one driving frequency being the initial value of the prepared odorant. In the quantification of a single component, only one type of olfactory receptor is needed. Here, the odorant sample used was 1-octen-3-ol and a type of olfactory receptor was Or13a. The response of the odorant sensor cells was expected to be nonlinear to concentration (S-shape curve), though the response was expected to increase monotonically with concentration excepting to extremely high concentrations. In other words, the responses of the target odorant and the prepared odorant were correlated with concentration. Fig. 3A shows the flowchart of the algorithm for the quantification of odorant concentrations. After initialization, the responses of the target odorant and the prepared odorant were measured, and the L2 norm of each response vector was compared. If the norm of the target odorant was larger, the concentration of the prepared odorant was updated to increase by one step. Conversely, when the norm of the target odorant was smaller, the concentration of the prepared odorant was updated to decrease by one step. As shown in Fig. 3B, only one measurement (i.e., $N = 1$) of the prepared odorant was required for a single concentration update. It is important to note that when there was no update point (i.e., when measuring the upper or lower limit of concentration), the concentration was not updated. The point to terminate the exploratory algorithm was set when the difference of the norm was within $\pm 0.5\%$. Although this is considered a strict condition, it allowed the algorithm's feasibility to be evaluated.

For quantification of the concentration of a binary mixture of odorants, the corresponding driving frequencies of the micro dispensers were 0, 30, and 100 Hz in which frequencies were combined to make nine combinations and one of the frequencies set as the target odorant. Compared to single component odorant quantification, binary component odorant quantification is more complicated. To determine the value of the target odorant concentration, a simplified adapted algorithm was used, based on downhill simplex method (Nelder and Mead, 1965) in which three points were measured. The number of measurement points is equal to the number of components plus one, which corresponds to $N = 3$ in Fig. 3A. The error norms of the target odorant vectors and the prepared odorant vectors at each of these three points were calculated, and the measurement point with the highest error was updated. Three measurement points were selected and taken from triangles which periodically arranged spaces as shown in Fig. 3C. Then, the measurement points were updated so that the triangle moved to adjacent simplex one after another. In other words, the point to be updated was moved to an adjacent triangle that shares the edge of the two non-updated points and was then updated to a new measurement point. For example, consider the case where the three points shown in blue in Fig. 3C are the measurement points. When the measurement point was updated due to the largest error of the measurement points whose driving frequencies of dispenser 1 and dispenser 2 are 30 and 30, respectively, the simplex was moved to measure the point at 0 and 0. In this setup, there were 9 points that could be measured, 8 ways to move a simplex consisting of 3 measurement points, and only a limited number of transition paths for the measurement points at the time of update. As an exception to the update rule, if the updated point was outside the defined area, the point was not updated and the point with the second largest error was updated. In addition, the termination condition of the exploratory algorithm was set to be when the measurement of the same simplex is repeated many times, or all 9 measurement points were measured.

3. Results and discussion

3.1. Reduction of photobleaching

When quantifying odorant concentration using active sensing, it is necessary to repeatedly measure and compare odorant responses. Previous research has confirmed that the fluorescence response values of odorant sensor cells gradually decay with prolonged measurement, referred to as photobleaching. To overcome photobleaching of the fluorescent protein and make it possible to repeatedly obtain odorant responses, it was necessary to reduce photobleaching. To do this, we first

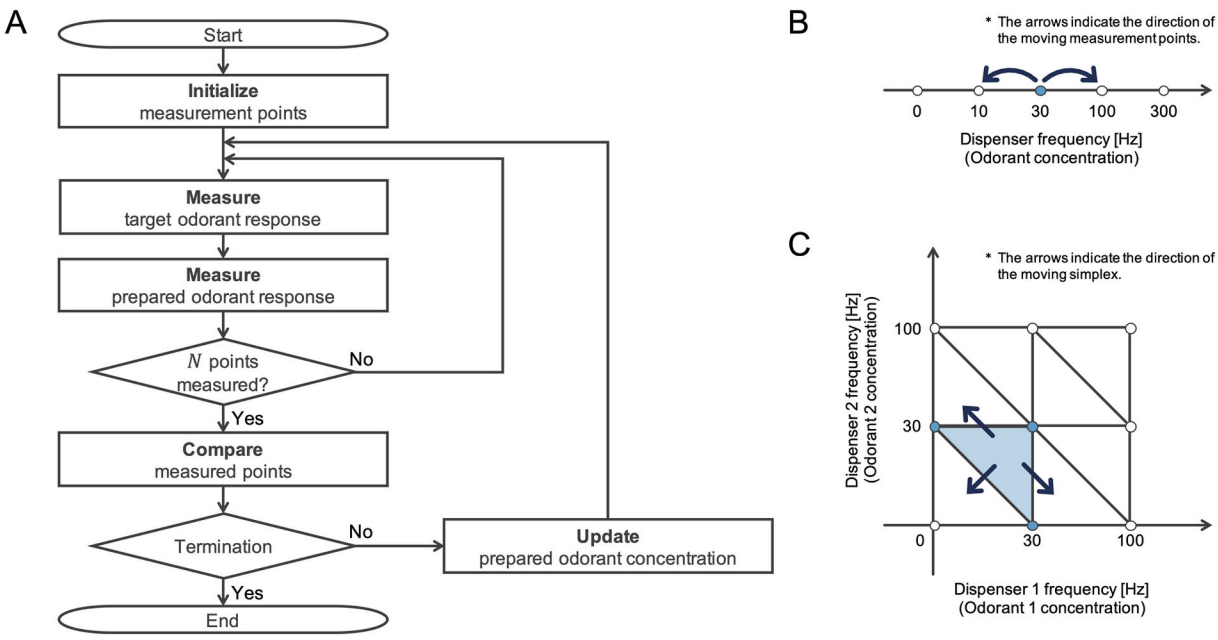

Fig. 3. Algorithm for updating the odorant concentration of the prepared odorant. A) Flow chart of the algorithm. In the case of one component, N = 1 point was measured and in the case of two components, N = 3 points were measured and evaluated for comparison. If the condition to terminate the algorithm was not met, the concentration of the prepared odorant was updated, and the measurement was conducted again. B) One-dimensional space of odor concentration in the quantification of the concentration of a single component. The relative odor concentration was selected from 0, 10, 30, 100, and 300 Hz based on the micro dispenser driving frequency. Based on the comparison between the prepared odorant response and the target odorant response, the concentration of the next prepared odorant was either increased or decreased. C) Two-dimensional space of odorant concentration in the quantification of binary component mixture odorant. The relative odorant concentrations of the two components were both selected from micro dispenser driving frequencies of 0, 30, and 100 Hz. From the three measurement points (blue points), the point with the largest error between the prepared odorant and the target odorant vectors were updated. (For interpretation of the references to colour in this figure legend, the reader is referred to the Web version of this article.)

confirmed photobleaching that was caused by excitation light through measurements of the odorant responses with strong and weak excitation light intensity and then compared the decay of the response values. The intensity of the excitation light was adjusted by pulse width modulation of the laser diode input current, with a duty ratio of 100% with high power excitation intensity and a duty ratio of 10% with low power excitation intensity. The basis for choosing an excitation intensity of 10% is related to the limitation of the laser diode module. When the intensity is decreased less than 10%, the excitation light becomes unstable. Therefore, 10% intensity was used as the weakest excitation power. In order to obtain fluorescence images with the same brightness at different excitation intensities, the exposure time of the image sensor and the image sampling period were adjusted in which images were taken at 10 frames per second with strong excitation intensity and 1 frame per second with weak excitation intensity. Only odorant sensor cells expressing Or13a were used. The odorant responses were measured when 1-octen-3-ol sample solution was applied five times repeatedly using a micro dispenser with a driving frequency of 100 Hz for 15 s at 345 s intervals.

Fig. 4 shows the comparison among the odorant responses when the intensity of the excitation light was changed under high power and low power conditions. The responses were normalized as the first response became 100%. Based on the *t*-test, though there were no statistically significant differences between strong and weak excitations in the second response, there were significant differences in the third, fourth, and fifth responses in which level of significance for this study was 0.05. Therefore, it cannot be said that the responses under the high and low power excitation intensities were the same. In other words, this supports the possibility that the weak excitation light may be able to suppress photobleaching with prolonged measurement. The coefficients of variation (CV) of the responses as shown in Fig. 4 were calculated for each trial in which odorants with the same concentration were measured repeatedly five times, and the average of CV for both the strong and

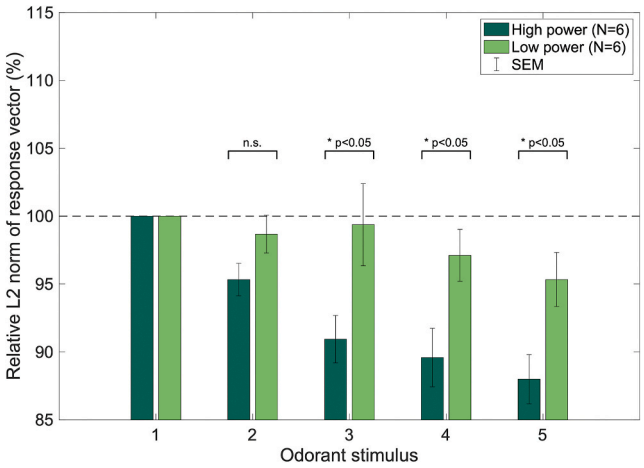

Fig. 4. The odorant responses were continuously measured five times under two different excitation light intensities. The odorant responses were calculated as the norm of the response vector and normalized to 100% of the average of the first time. Error bars indicate standard error of the mean. The number of measurements in both the high power and low power conditions was N = 6.

weak excitation light intensity was calculated. As a result, the average CVs for strong and weak excitation light intensities were 0.054, and 0.032, respectively. Thus, decreasing the excitation light intensity is efficient in reducing CV.

However, it is important to note that even under weak excitation light intensity, the fifth odorant response declined compared to the first response. It is necessary to reduce the excitation intensity as low as possible, though this becomes a trade-off between the suppression of photobleaching and the exposure time of the fluorescent image. It is also

important to note that intermittent excitation, in which the emittance of excitation light is stopped when not evaluating responses, was not considered to be appropriate as the fluorescence of the odorant sensor cells require time to be stabilized after turning on the excitation light. Although previously these measurements were difficult, the repeated measurements required for active sensing became feasible after adjusting the excitation power.

Furthermore, a preliminary experiment was conducted in which odorant responses were measured 20 times repeatedly with weak excitation intensity. Though the odorant response and signal baseline values were gradually decreased due to photobleaching, the response value never reached 0. Therefore, decreasing the excitation light intensity allows us to increase the precision level of repeated measurement for odorant quantification.

The reason that the response intensity gradually decreases is related to photobleaching according to the result in Fig. 4. As all the cells in the image change at the same time due to photobleaching, the relative response to odorants is also influenced uniformly. Thus, the influence of photobleaching can be reduced through active sensing and real-time reference method. Moreover, the difference between individual cells can be reduced as an adequate number of cell (200–400 cells in the image) are used as a sensor array. Therefore, reliability of the response data of the cells are deemed to be enough.

3.2. Single component odorant quantification

The measurement system enabled the volume and consequently concentration of the odorant samples fed to the odorant sensor cells to be controlled by changing the driving frequency of the micro dispenser. Prior to the quantification of the single component odorant concentration, it was confirmed that odorant response is dependent on the driving frequency of the micro dispenser (results not shown). To do this, Or13a sensor cells were used and 1-octen-3-ol solution was injected into the measurement chamber with 0 Hz–300 Hz of the driving frequency of the micro dispenser. This resulted in the confirmation of the concentration-dependent response.

Following this, the quantification of single component odorant concentration was then tested. In this experiment, the concentration of the target odorant was set to 100 Hz at the micro dispenser driving frequency, whereas the initial value of the concentration of the prepared odorant was set to 0 Hz. Both the target and the prepared odorants were supplied from the same micro dispenser. Based on the single component exploratory algorithm, the target odorant or the prepared odorant were supplied every 6 min for 15 s and fed until the termination condition was met. Based on the results of the previous section, the relative intensity of the excitation light was 10%, and the image sampling period was 4 s. This sampling period was slow enough to conduct real-time image processing.

Fig. 5 shows the transitions of the L2 norm of the response vectors for the odorant responses to the target odorant and the prepared odorant. The dimension of the response vector was 235 which was equal to the number of detected sensor cells in the image. The first comparison between the target odorant and the prepared odorant shows that the norm of the prepared odorant is clearly smaller than that of the target odorant. Therefore, as per the algorithm, the second prepared odorant's concentration was increased by one step. Since the prepared odorant responses were small until the third comparison, the concentration was increased step by step. In the fourth comparison, the difference between the norm of the response vectors was considerably smaller than in the first three comparisons and the concentration of the prepared odorant was the same as that of the target odorant. However, as the condition for the termination of the algorithm had not been met, this resulted in the concentration being decreased as the response of the prepared odorant became slightly larger. In the fifth comparison, the concentration was again increased as the prepared odorant response was low. In the sixth comparison, the concentration was again the same, but similar to the

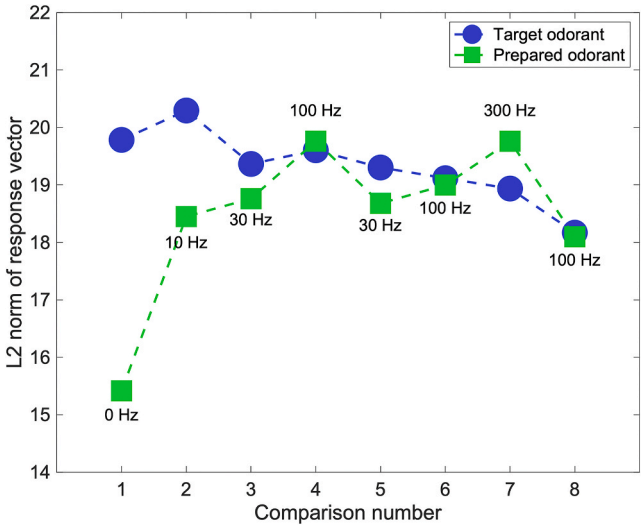

Fig. 5. Transition of the norm of the response vectors for target and prepared odorants in the quantification of single component odorant concentration. The concentration of the target odorant was 100 Hz at the micro dispenser driving frequency. The micro dispenser driving frequencies for the prepared odorants are given in the graph.

fourth comparison, the algorithm stopping condition were not met. However, this time the concentration was increased as the prepared odorant response was small. In the seventh comparison, the concentration was decreased as the prepared odorant registered a response that was clearly larger than the target odorant. The eighth time was the same concentration as the third time, but because the response values were close enough to meet the termination condition, the quantification was terminated. The convergence around 100 Hz was observed after fourth measurement. Thus, this confirmed that it is possible to use a sensor system with an algorithm such as the one described above in order to match the concentrations of a target odorant and a prepared odorant.

In Fig. 5, when looking at the transitions of the response vector norms of the target odorant, it can be seen that in spite of measuring the same concentration, the response vector norms fluctuated and ultimately decreased. This increase and decrease of response values are thought to be related to the fluctuation of the odorant sensor cells themselves. In addition, an overall negative downward trend in the response values throughout the whole process is thought to be possibly related to photobleaching. Each odor measurement lasted for 6 min in which we continued to measure for 96 min until the completion of eight comparisons. Since this is a prolonged measurement, the influence of photobleaching may occur even when using weak excitation light. However, despite a decrease in the response values, the comparison between the norm of the target and prepared odorants all corresponded to the actual magnitude relationship between the odorant concentrations given. This is thought to be related to the fact that the target odorant was re-measured at each comparison by the real-time reference method. The single component quantification successfully worked even if gradual decrease in sensor sensitivity owing to photobleaching occurred.

3.3. Binary mixture odorant quantification

Quantification of binary mixture odorant concentration was performed. The micro dispensers driving frequencies for the target odorant were set to 100 Hz for both of geosmin and 1-octen-3-ol. For simplicity, the concentrations of geosmin and 1-octen-3-ol will be referred to by their micro dispensers driving frequencies, for example the target odorant is represented by (100, 100). For the algorithm, the prepared odorants were measured at three points in which the initial values were

(0, 0), (30, 0), and (0, 30). The odorant samples were supplied in the same manner as in the quantification of a single component odorant concentration and were fed for 15 s every 6 min. The sampling period of the image was also 4 s.

Fig. 6 shows the results of the state transitions during the quantification of the odorant concentration in the above conditions. The dimension of the response vector was 337 which was used to calculate the error of target and prepared odorant vectors. Fig. 6A shows the transitions of the errors at the measurement points of the three prepared odors while Fig. 6B shows each transition for the measured points in the two-dimensional odorant concentration space. Table 1 shows a summary of the update epoch transition.

First, three initial points were measured, and the norm of the error vector compared to the target odorant for each of them was determined. With (0, 0) having the largest error, this point was updated, and the concentration changed to (30, 30). The first update epoch then compared (30, 0) and (0, 30) which were initially measured, and (30, 30) which were newly measured points. Point (30, 0) had the largest error which was then updated to point (0, 100). In this manner, the point that had the largest error was updated one after another if the point could be updated as seen in update epoch two to four. In the fifth update epoch, the points (30, 100), (100, 30), and (100, 100), which included the same concentration as the target odorant were measured. Though the point with the smallest error was (100, 100), since the other points could not be updated, the point (100, 100) was updated to (30, 30) in update epoch six. On the seventh update epoch, all nine measurable concentrations were finally measured, and the exploratory algorithm was terminated. From the above result, it was concluded that a simplex composed of three prepared odorants gradually shifted to the same concentration as the target odorant. In Fig. 6A, the point with the smallest error among the nine measurement points was the same as that of the target odorant. Thus, the binary quantification was successful.

The exploratory algorithm successfully found the target odorant as the smallest error of the measured points. Experimental trials have confirmed that the concentration of the prepared odorant reached the same concentration of the target odorant more than once in addition to the result shown in Fig. 6. Furthermore, the real-time reference method reduced the influence of temporal fluctuation when comparing the response values of the prepared odorant and the target odorant. However, there was a contradiction in the order of the magnitude of error values for the measurement points in the fourth and sixth update epochs.

Table 1
Summary of the update epoch transition.

Update epoch 0 to 1:	(0, 0)	→	(30, 30)
Update epoch 1 to 2:	(30, 0)	→	(0, 100)
Update epoch 2 to 3:	(0, 30)	→	(30, 100)
Update epoch 3 to 4:	(0, 100)	→	(100, 30)
Update epoch 4 to 5:	(30, 30)	→	(100, 100)
Update epoch 5 to 6:	(100, 100)	→	(30, 30)
Update epoch 6 to 7:	(30, 100)	→	(100, 0)

This may be related to the state of the sensor cells and variation in the environment of the measurement system following prolonged measurement. Measurement was taken 20 times until the algorithm was terminated after 120 min. In other words, the contradiction occurred due to the algorithm comparing three points measured at three different times. Also, cell viability may become a problem as the iteration of measurement increases. The quantification time required for the algorithm in this research depends on the number of update epochs which is determined by the initial concentrations of the prepared odorant as the route in the concentration space that the update algorithm can use is limited. However, the contradiction problem and cell viability problem can be mitigated by introducing more efficient quantification algorithm to reduce the number of repetitions. Furthermore, in this study, mixture quantification was carried out under the assumption that only a few set of concentrations of odorants existed. This is significantly different from real life in which there are an indeterminable number of odorants all with varying concentrations in the world. Further refinement of the response evaluation method in order to suppress the influence of sensor response fluctuation and to more efficiently compare responses may allow for higher resolution of odorant concentrations. In addition, this measurement system allowed for the determination of the relative concentration of odorants. The development of a method for determining the absolute values of concentrations should be further studied.

4. Conclusions

In this study, an odor biosensor system using an array of odorant sensor cells combined with an active sensing method was developed, and the quantification of odorants with one or two components were successfully demonstrated. It was confirmed that the system was capable

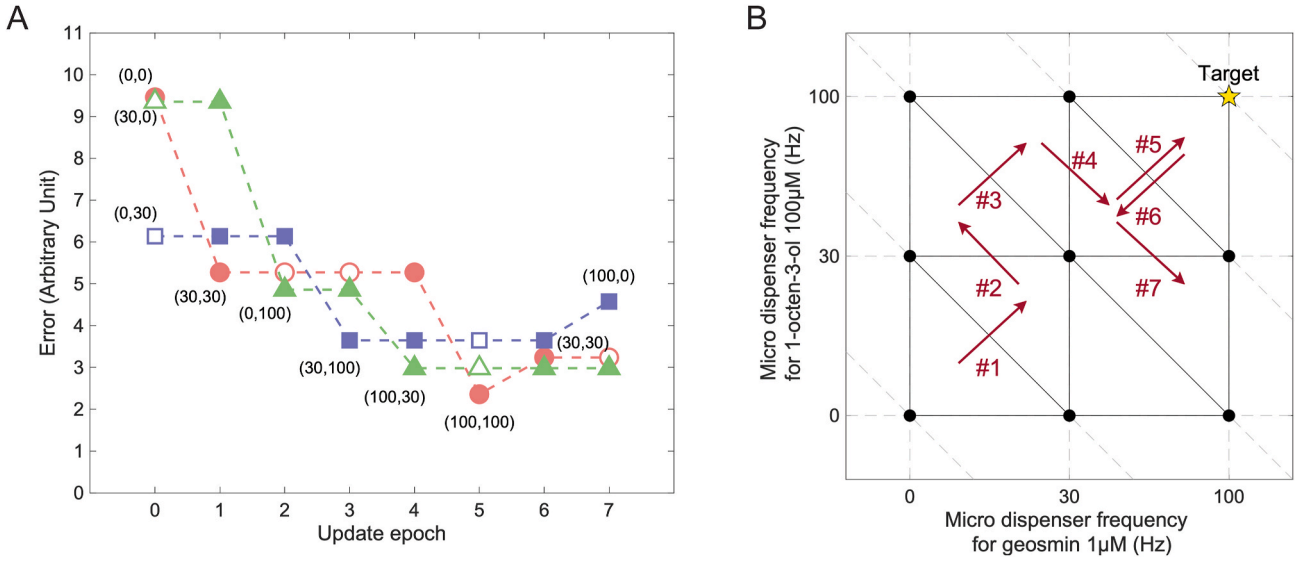

Fig. 6. State transitions of the exploratory algorithm in the quantification of binary mixture odorant concentration. A) Transition of the magnitude of error in the response vectors of the target and prepared odorant for each concentration update. The markers that are filled in are updatable, and the unfilled markers are not updatable. B) Transition at each concentration update of a triangle simplex. A star marker indicates the concentration of the target odorant.

of quantifying odorant concentrations with not only one component, but also binary component mixtures through repeated comparison of responses and modifying the prepared odorant. The influence of the cells' response fluctuations over prolonged measurement was mitigated by comparing responses of the target odorant and the prepared odorant using a real-time reference method. This study attempted to quantify odorant concentrations by using a sensor array of the biosensor with active sensing. To the best of our knowledge, the mixture quantification method using odor biosensor with active sensing is a new and novel method, and we believe that it demonstrates a new direction for odor biosensors.

On the other hand, our method is not able to quantify absolute concentrations, but rather only relative concentration can be determined. In order to quantify the absolute concentrations, a calibration mechanism needs to be built into the system. The algorithm used in this study is still primitive and was only successful due to the limited number of odorant components. While the ability to quantify the concentrations of multiple odorants will have greater application, this research was conducted to explore the use of the sensor array of the odorant biosensor for the first time. In other words, we focused on developing proof of concept in which we adopted 2 types of olfactory receptors and measured odorants mixed with 2 types of odorants. More appropriate algorithms to quantify more components will need to be developed. In order to apply optimization methods such as gradient descent method, it will be necessary to increase the resolution of odorant concentration in order to calculate the gradient of error in the odorant concentration space. In addition, we believe that the measurable odorant space can be extended by increasing the number of olfactory receptors used. Although the results of this study were obtained under limited conditions and there are many challenges that need to be addressed, we believe that this research paves the way for the development of odor biosensors that can be used in various applications including odor recorders.

CRediT authorship contribution statement

Yuji Sukekawa: Methodology, Software, Formal analysis, Investigation, Writing - original draft, Visualization, Funding acquisition. **Hidefumi Mitsuno:** Methodology, Investigation, Resources, Writing - review & editing. **Ryohei Kanzaki:** Methodology, Resources, Writing - review & editing. **Takamichi Nakamoto:** Conceptualization, Methodology, Writing - review & editing, Project administration, Funding acquisition.

Declaration of competing interest

The authors declare that they have no known competing financial interests or personal relationships that could have appeared to influence the work reported in this paper.

Acknowledgements

This work was partially supported by JSPS KAKENHI under Grant JP17J10158 and Grant JP18H03773.

Appendix A. Supplementary data

Supplementary data to this article can be found online at https://doi.org/10.1016/j.bios.2021.113053.

References

Carey, W.P., Beebe, K.R., Kowalski, B.R., 1987. Multicomponent analysis using an array of piezoelectric crystal sensors. Anal. Chem. 59, 1529–1534. https://doi.org/10.1021/ac00138a010.

Chen, T.-W., Wardill, T.J., Sun, Y., Pulver, S.R., Renninger, S.L., Baohan, A., Schreiter, E. R., Kerr, R. a, Orger, M.B., Jayaraman, V., Looger, L.L., Svoboda, K., Kim, D.S., 2013. Ultrasensitive fluorescent proteins for imaging neuronal activity. Nature 499, 295–300. https://doi.org/10.1038/nature12354.

Figueroa, X.A., Cooksey, G.A., Votaw, S.V., Horowitz, L.F., Folch, A., 2010. Large-scale investigation of the olfactory receptor space using a microfluidic microwell array. Lab Chip 10, 1120–1127. https://doi.org/10.1039/b920585c.

Galizia, C.G., Munch, D., Strauch, M., Nissler, A., Ma, S., 2010. Integrating heterogeneous odor response data into a common response model: a DoOR to the complete olfactome. Chem. Senses 35, 551–563. https://doi.org/10.1093/chemse/bjq042.

Gutierrez-Osuna, R., 2002. Pattern analysis for machine olfaction: a review. IEEE Sensor. J. 2, 189–202. https://doi.org/10.1109/JSEN.2002.800688.

Hsieh, Y.-C., Yao, D.-J., 2018. Intelligent gas-sensing systems and their applications. J. Micromech. Microeng. 28, 093001 https://doi.org/10.1088/1361-6439/aac849.

Khadka, R., Aydemir, N., Carraher, C., Hamiaux, C., Colbert, D., Cheema, J., Malmström, J., Kralicek, A., Travas-Sejdic, J., 2019. An ultrasensitive electrochemical impedance-based biosensor using insect odorant receptors to detect odorants. Biosens. Bioelectron. 126, 207–213. https://doi.org/10.1016/J.BIOS.2018.10.043.

Ko, H.J., Park, T.H., 2005. Piezoelectric olfactory biosensor: ligand specificity and dose-dependence of an olfactory receptor expressed in a heterologous cell system. Biosens. Bioelectron. 20, 1327–1332. https://doi.org/10.1016/j.bios.2004.05.002.

Lee, S.H., Oh, E.H., Park, T.H., 2015. Cell-based microfluidic platform for mimicking human olfactory system. Biosens. Bioelectron. 74, 554–561. https://doi.org/10.1016/j.bios.2015.06.072.

Liu, Q., Ye, W., Hu, N., Cai, H., Yu, H., Wang, P., 2010. Olfactory receptor cells respond to odors in a tissue and semiconductor hybrid neuron chip. Biosens. Bioelectron. 26, 1672–1678. https://doi.org/10.1016/J.BIOS.2010.09.019.

Marco, S., Gutierrez-Galvez, A., 2012. Signal and data processing for machine olfaction and chemical sensing: a review. IEEE Sensor. J. 12, 3189–3214. https://doi.org/10.1109/JSEN.2012.2192920.

Mitsuno, H., Sakurai, T., Namiki, S., Mitsuhashi, H., Kanzaki, R., 2015. Novel cell-based odorant sensor elements based on insect odorant receptors. Biosens. Bioelectron. 65, 287–294. https://doi.org/10.1016/j.bios.2014.10.026.

Mujiono, T., Sukekawa, Y., Nakamoto, T., Mitsuno, H., Termtanasombat, M., Kanzaki, R., Misawa, N., 2017. Sensitivity improvement by applying lock-in technique to fluorescent instrumentation for cell-based odor sensor. Sensor. Mater. 29, 65–76. https://doi.org/10.18494/SAM.2017.1378.

Münch, D., Galizia, C.G., 2016. DoOR 2.0 - comprehensive mapping of Drosophila melanogaster odorant responses. Sci. Rep. 6, 21841. https://doi.org/10.1038/srep21841.

Murugathas, T., Zheng, H.Y., Colbert, D., Kralicek, A.V., Carraher, C., Plank, N.O.V., 2019. Biosensing with insect odorant receptor nanodiscs and carbon nanotube field-effect transistors. ACS Appl. Mater. Interfaces 11, 9530–9538. https://doi.org/10.1021/acsami.8b19433.

Nakamoto, T., 2016. Olfactory display and odor recorder. In: Nakamoto, T. (Ed.), Essentials of Machine Olfaction and Taste. John Wiley & Sons Singapore Pte Ltd, Singapore, pp. 247–314. https://doi.org/10.1002/9781118768495.ch7.

Nelder, J.A., Mead, R., 1965. A simplex method for function minimization. Comput. J. 7, 308–313. https://doi.org/10.1093/comjnl/7.4.308.

Olsson, M.J., Lundström, J.N., Kimball, B.A., Gordon, A.R., Karshikoff, B., Hosseini, N., Sorjonen, K., Olgart Höglund, C., Solares, C., Soop, A., Axelsson, J., Lekander, M., 2014. The scent of disease: human body odor contains an early chemosensory cue of sickness. Psychol. Sci. 25, 817–823. https://doi.org/10.1177/0956797613515681.

Olsson, S.B., Challiss, R.A.J., Cole, M., Gardeniers, J.G.E., Gardner, J.W., Guerrero, A., Hansson, B.S., Pearce, T.C., 2015. Biosynthetic infochemical communication. Bioinspiration Biomimetics 10, 043001. https://doi.org/10.1088/1748-3190/10/4/043001.

Son, M., Kim, D., Ko, H.J., Hong, S., Park, T.H., 2017. A portable and multiplexed bioelectronic sensor using human olfactory and taste receptors. Biosens. Bioelectron. 87, 901–907. https://doi.org/10.1016/j.bios.2016.09.040.

Stensmyr, M.C., Dweck, H.K.M., Farhan, A., Ibba, I., Strutz, A., Mukunda, L., Linz, J., Grabe, V., Steck, K., Lavista-Llanos, S., Wicher, D., Sachse, S., Knaden, M., Becher, P. G., Seki, Y., Hansson, B.S., 2012. A conserved dedicated olfactory circuit for detecting harmful microbes in Drosophila. Cell 151, 1345–1357. https://doi.org/10.1016/j.cell.2012.09.046.

Sukekawa, Y., Mitsuno, H., Kanzaki, R., Nakamoto, T., 2019. Odor discrimination using cell-based odor biosensor system with fluorescent image processing. IEEE Sensor. J. 19, 7192–7200. https://doi.org/10.1109/JSEN.2019.2916377.

Sundgren, H., Winquist, F., Lundström, I., 1991. Artificial neural networks and statistical pattern recognition improve MOSFET gas sensor array calibration. Transducers '91 574–577. https://doi.org/10.1109/sensor.1991.148942.

Sung, J.H., Ko, H.J., Park, T.H., 2006. Piezoelectric biosensor using olfactory receptor protein expressed in Escherichia coli. Biosens. Bioelectron. 21, 1981–1986. https://doi.org/10.1016/j.bios.2005.10.002.

Termtanasombat, M., Mitsuno, H., Misawa, N., Yamahira, S., Sakurai, T., Yamaguchi, S., Nagamune, T., Kanzaki, R., 2016. Cell-based odorant sensor array for odor discrimination based on insect odorant receptors. J. Chem. Ecol. 42, 716–724. https://doi.org/10.1007/s10886-016-0726-7.

Vergara, A., Llobet, E., Brezmes, J., Ivanov, P., Cané, C., Gràcia, I., Vilanova, X., Correig, X., 2007. Quantitative gas mixture analysis using temperature-modulated micro-hotplate gas sensors: selection and validation of the optimal modulating frequencies. Sensor. Actuator. B Chem. 123, 1002–1016. https://doi.org/10.1016/j.snb.2006.11.010.

Wang, Z., Kowalski, B.R., Hwang, J.N., Wang, Z., 1995. ChemNets: theory and application. Anal. Chem. 67, 1497–1504. https://doi.org/10.1021/ac00105a003.

Wu, C., Du, L., Wang, D., Wang, L., Zhao, L., Wang, P., 2011. A novel surface acoustic wave-based biosensor for highly sensitive functional assays of olfactory receptors. Biochem. Biophys. Res. Commun. 407, 18–22. https://doi.org/10.1016/J.BBRC.2011.02.073.

Yamanaka, T., Matsumoto, R., Nakamoto, T., 2003. Fundamental study of odor recorder for multicomponent odor using recipe exploration method based on singular value decomposition. IEEE Sensor. J. 3, 468–474. https://doi.org/10.1109/JSEN.2003.815778.

Yamanaka, T., Nakamoto, T., 2003. Real-time reference method in odor recorder under environmental change. Sensor. Actuator. B Chem. 93, 51–56. https://doi.org/10.1016/S0925-4005(03)00202-8.